

THERMOMECHANICS OF PV MODULES INCLUDING THE VISCOELASTICITY OF EVA

Ulrich Eitner^{1,*}, Matthias Pander², Sarah Kajari-Schröder¹, Marc Köntges¹ and Holm Altenbach³

¹Institute for Solar Energy Research Hamelin (ISFH), Am Ohrberg 1, D-31860 Emmerthal, Germany

²Fraunhofer Center for Silicon Photovoltaics, Walter-Huelse-Strasse 1, D-06120 Halle (Saale), Germany

³Martin-Luther University Halle-Wittenberg, Kurt-Mothes-Strasse 1, D-06099 Halle (Saale), Germany

*now with Fraunhofer Institute for Solar Energy Systems ISE, Heidenhofstraße 2, 79110 Freiburg, Germany

ABSTRACT: We quantify the thermomechanical stresses in a crystalline photovoltaic module during thermal cycling between -40°C and 85°C with the help of a Finite-Element-Analysis of a 60 cell module. The quality of the simulation model is verified by a comparison to displacement experiments where the thermomechanical deformation of solar cells in a PV laminate is measured [1]. We find that the key feature in the simulation model is the viscoelastic material model for the EVA-encapsulant in order to obtain a good agreement with the experiments. The simulated stresses in the solar cells at -40°C are compressive and reach values of up to 75 MPa. In contrast, the back sheet is at -40°C under tensile stress of 45 MPa while the 4 mm thick glass experiences very low stresses. The EVA deforms with principal strains of up to 23% which proves the EVA's mechanical function as a compliant buffer layer. The change in the distance between two solar cells depends on their position in the module: close to the center the gap change is $120\ \mu\text{m}$ (150°C to -40°C) while at the module edges the change in the cell distance is $170\ \mu\text{m}$.

Keywords: PV module, Encapsulation, Simulation, Reliability, Mechanics

1 INTRODUCTION

Nowadays module manufacturers face the challenge to integrate thinner solar cells [2], cells with both contacts at the rear side [3] and the task to further reduce the module cost. In order to face these challenges and maintaining the demanding module warranties of 25 years at the same time, the limits of the standard module design or solutions beyond the conventional module designs have to be explored [4, 5]. It is therefore essential to understand the thermomechanics, i.e. the build-up of stresses from thermal and mechanical loads, when developing new module concepts or when preparing existing concepts for novel and potentially more fragile cell structures. As mechanical failure is related to stress and strain these quantities need to be investigated to improve the module design. Even in today's conventional crystalline modules high mechanical stress may cause cracks in the solar cells, which have been shown to lead to a reduced long time stability of PV-module power [6], or interconnect failures, that dramatically affect the module performance. As an example, the impact of the mechanical load test in the IEC 61215 on the formation of cracks is studied by Kajari-Schröder [7], showing a relation between crack formation and bending strains in the module.

This work presents the completion of a number of preliminary experimental and modeling investigations performed at the ISFH aiming to determine the thermo-mechanical stress and strain in a PV module. In 2008, we presented the FEM-simulation of a laminated string [8] using only linear elastic material models. However, experiments were needed to assess the quality of the simulation. In 2009, we successfully transferred the method of digital image correlation to the field of PV module technology in order to measure the deformation of laminated solar cells contactless. We determined that the gap between two solar cells deforms with approximately $0.5\ \mu\text{m}/^{\circ}\text{C}$ [1]. An analysis of the accuracy of this digital image correlation method led to $\pm 1.14\ \mu\text{m}$ [9]. The same method was used by Meier [10] at the Fraunhofer CSP to inspect copper ribbons in PV modules. In 2010, we presented a viscoelastic material

model for EVA based on a generalized Maxwell model [11]. The Maxwell parameters were determined from tensile relaxation and creep experiments [12]. Pander [13] recently demonstrated that simulations with a similar viscoelastic model for EVA were in good agreement with the experimental results in [10].

We now use the viscoelastic model for EVA along with linear elastic models for the other module materials to simulate the gap experiments. Furthermore, we compare the EVA-models of linear elasticity and of temperature-dependent linear viscoelasticity to the experimental data. The model most consistent with the experiment is then chosen for a FEM-simulation of a 60-cell module in order to answer the central questions of thermomechanics of PV modules: How high are the mechanical stresses in the cells? Is the position of a solar cell in the module relevant for the stress in the cell? How large is the change in the distance between two adjacent solar cells and is it identical for all gaps in the module?

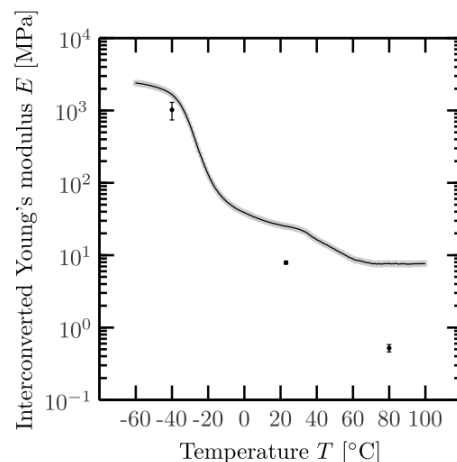


Figure 1: Dynamic mechanical analysis of EVA. The shear data are interconverted to tensile data. The dots indicate the Young's modulus obtained from tensile tests at isothermal temperatures.

2 MATERIAL MODELS FOR EVA

From experiments of cured EVA samples we found the mechanical properties to depend on time and on temperature [11]. However, to keep the simulation complexity at the lowest possible level for the simulation of the thermomechanical behaviour of PV laminates, we evaluate three different material models for EVA (increasing complexity from 1 to 3) and compare them to the experimental data measured in [1]:

1. linear elasticity
2. temperature-dependent linear elasticity
3. linear viscoelasticity

Figure 1 shows a Dynamic mechanical analysis (DMA) of cured EVA. A linear elastic model can only take into account a constant value for the elastic modulus. We thus use the highest (2.1 GPa) and lowest value (6.5 MPa) of the Young’s modulus for the EVA to construct two extremal linear elastic models.

The temperature-dependent linear elastic model uses the complete curve shown in Fig.1 to express the Young’s modulus as a function of the temperature.

The viscoelastic model for EVA is constructed from tensile relaxation and creep experiments as described in [11] and [12].

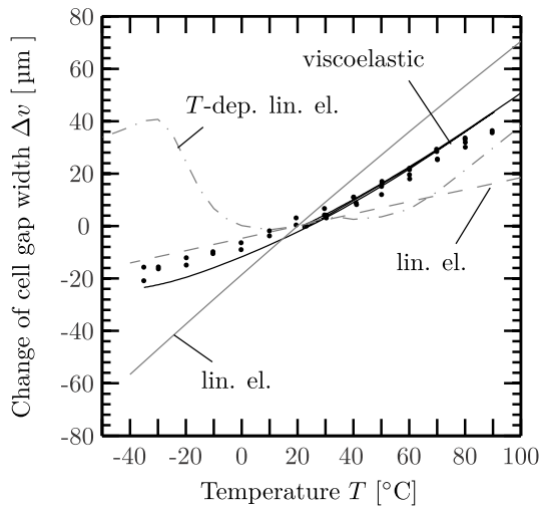


Figure 2: Experimental change of the distance between two adjacent solar cells (dots) and the FEM-simulations with different material models for EVA (taken from [14]).

Figure 2 shows the experimental data published in [1], where the gap displacement of a laminate with 3 non-interconnected cells is measured. The simulated experiments using the three different models for EVA are plotted as lines.

The linear elastic simulations give straight lines in Fig. 2 while the temperature-dependent model deviates strongly from the experimental data, especially at cold temperatures. What looks physically unlikely is due to our method to compare the simulation to the experiment: the simulated curves are shifted to zero gap displacement at 25°C. The simulated *T*-dependent curve is bounded by the two linear elastic curves when inspecting only the simulation with zero gap displacement at 150°C. We find

the viscoelastic material model of EVA to give the best agreement with the measured data. It also reproduces the characteristic shape of the experimental data which resembles a slightly curved parabola.

3 FEM-SIMULATION OF A PV-MODULE

The model describes a frameless 60 cell module without interconnects. The cell size is 125 mm × 125 mm pseudo-square. The symmetry of the module is exploited by modelling only the lower left hand quarter of the complete module. We assume a stress-free initial state at 150°C lamination temperature where the materials are bonded together. The initial thickness of each layer is given in Table 1 as well as the mechanical material parameters. The solar cells are modelled with bulk silicon properties taking into account the cubic symmetry, where the edges are (100)-oriented. The model is 3D with continuum elements.

Table 1: Input parameters for FEM-simulation (for details see [12])

	Thickness [μm]	Young’s modulus [GPa]	CTE [10 ⁻⁶ 1/K]
Glass	4000	73	8
Back sheet	350	3.5	50.4
EVA	500	viscoelastic	270
Solar cells	200	anisotropic	<i>T</i> -dep.

When the module cools down from the initial stress-free state at 150°C the material assembly contracts. At -40° C we find the stresses at the outer glass surface to be compressive with the first principal stress σ_1 between 0 MPa and 12 MPa. In contrast, the back sheet on the other outer face is in high tension so that the first principal stress reaches up to 41 MPa (Fig. 3).

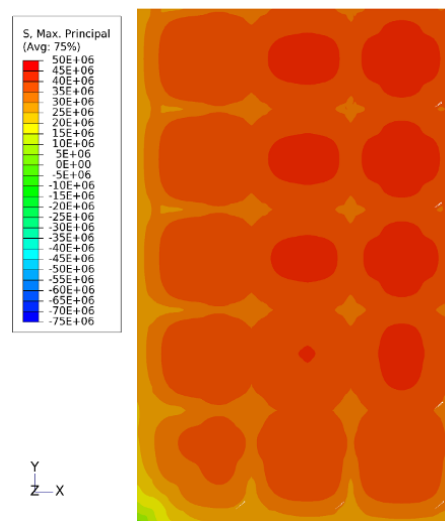


Figure 3: First principal stress σ_1 in the back sheet with tensile stress values between 0 and 41 MPa (taken from [14]). Lower left hand quarter of the module is shown.

The embedded solar cells are under high compressive stress which is visualized in Fig. 4 by the third principal stress σ_{III} ranging from -74 MPa to -16 MPa. In the solar cells the in-plane stresses are one to two orders of magnitude higher than the out-of-plane stress components, which are thus not shown here. Large strains are present in the EVA at -40°C exceeding 20% in the first principal strain ϵ_1 .

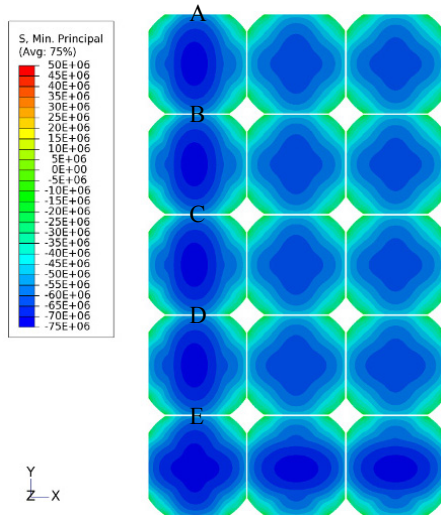


Figure 4: Third principal stress σ_{III} in the solar cells with compressive stress values between -74 MPa and -16 MPa (taken from [14]). Lower left hand quarter of the module is shown.

Figure 5 shows the displacement of the gap between two cells. The letters indicate the positions of the gaps in the module as shown in Fig. 3. The change of the gap width is lowest for cells in the center of the module (-130 μm) and highest for cells at the edge (-175 μm). The curves exhibit an offset at 25°C which is largest for gap E with 5 μm implying that the cells drift apart from each other during a temperature cycle. This is due to the viscoelasticity of EVA, as all other materials deform reversibly and independent of time according to their implemented material models.

4 CONCLUSIONS

The module contracts when it cools down from a stress-free lamination temperature. This deformation mode is maintained during a subsequent thermal cycle. The glass makes 70% of the module thickness and dominates the deformation which follows the thermal contraction according to the CTE of glass. The back sheet has a higher CTE than glass. Therefore the back sheet can not contract as much as in free configuration and is consequently under tensile stress. The cells in between these two layers exhibit the lowest CTE and are thus under compression with up to -74 MPa stress at -40°C. The cells at the edges are more stressed than interior cells. The EVA is very compliant and exhibits large strains, which illustrates its function as a compliant buffer layer.

The gap between adjacent solar cells decreases by 130 μm between 150°C and -40°C for cells close to the

module center and by 175 μm for cells at the module edge. The optimal shape of interconnects should thus be designed to withstand a maximum gap displacement of up to 175 μm without fatigue failure and without introducing high stresses into the cells.

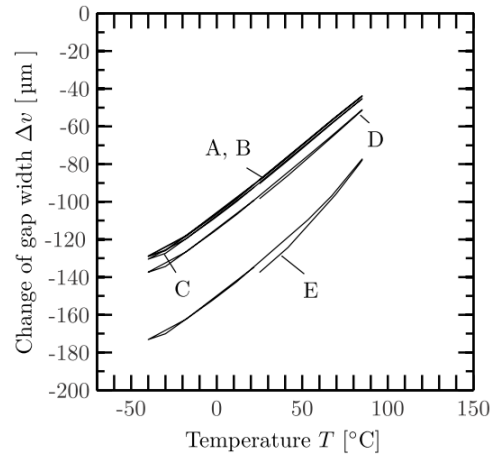


Figure 5: Simulated gap displacement between two solar cells in a PV module. The letters indicate the position in the module in Fig.4. The interconnectors are thus most stressed at the cells closest to the module edge.

5 ACKNOWLEDGEMENTS

The authors thank Professor Brendel for his support of this work. Funding was provided by the State of Lower-Saxony.

6 REFERENCES

- [1] U. Eitner et al, Proc. 34th IEEE PVSC (2009), pp.1280-1284
- [2] J. Wohlgemuth et al, Proc. 33rd IEEE PVSC (2008), pp.1-4
- [3] E.V. Kerschaver et al, Prog. in PV 14 (2006), pp.107-123
- [4] P. de Jong, Photovoltaics International 7 (2010), pp.138-144
- [5] J. Gee, Proc. 34th IEEE PVSC (2009), pp.2133-2137
- [6] M. Köntges et al, Sol. Eng. Mat. 95 (2011), pp.1131-1137
- [7] S. Kajari-Schröder et al. Sol. Eng. Mat. 95 (2011), pp.3054-3059
- [8] U. Eitner et al, Proc. 23rd EUPVSEC (2008), pp.2815-2817
- [9] U. Eitner et al, Sol. Eng. Mat. 94 (2010), pp.1346-1351
- [10] R. Meier et al, Proc. 25th EUPVSEC (2010), pp.3740-3744
- [11] U. Eitner et al, Proc. 25th EUPVSEC (2010), pp.4366-4368
- [12] U. Eitner, PhD Thesis, Martin-Luther-University Halle-Wittenberg, 2011
- [13] M. Pander et al., Proc. 12th EuroSimE (2011)
- [14] Eitner et al., in: Shell-like structures, Advanced structural materials 15(5), Springer (2011), p.453-468